SHORT FATIGUE CRACK GROWTH BEHAVIOUR IN PLAIN BEARINGS

M.R. Joyce*, S. Syngellakis** and P.A.S. Reed*, Department of Engineering Materials* and Department of Mechanical Engineering**, University of Southampton, Highfield, Southampton, SO17 1BJ, UK

INTRODUCTION

Plain bearings have been in use for many years, over this time their design and the choice of materials used in their construction has been continuously improved. They are currently used as main and con-rod big end bearings in automotive engines. The service conditions for automotive bearings are becoming more severe with new engine designs, and it is important that new bearing materials are designed to provide the longest possible operating life at these higher loads, and at an economic cost. In order to do this it is necessary to study both the loading conditions and the fatigue failure behaviour of plain bearings, with a view to optimising their design and the use of appropriate materials. The aim of our research is to evaluate early fatigue initiation and short crack growth behaviour in bearing materials to establish the key parameters controlling early crack propagation, hence providing material optimisation data. The approach taken combines experimental fatigue evaluation of the bearing lining and finite element modelling of the local microstructure.

Bearing Materials and Design

This paper reports the results of an investigation on a relatively simple bearing design. The bearing consists of two half shells, which are clamped together in the housing to support the journal. Each half shell contains a number of layers of different material. The bearing lining (~0.25mm) material is an Al-Si-Sn alloy, which is bonded to a steel backing layer (~1.5mm) by a thin layer of pure Al foil (~ 60μm). The Al layer is also used to prevent Sn diffusing into the steel and causing embrittlement.

Fatigue Behaviour

Fatigue behaviour of automotive bearings is dependent on many complex factors. Plain bearings are loaded via the oil layer separating the bearing surface from the journal. The behaviour of this hydrodynamic oil film causes discontinuous and rapidly changing stress fields to be set up across the bearing surface. Coupled with a multi-layer material system this loading gives rise to complex fatigue behaviour, characterised by multiple crack initiations and coalescence as observed by Shenton et al [1].

METHODOLOGY

Most fatigue optimisation studies to date have used artificial accelerated test techniques using rigs which aim to simulate the loading regime within an engine, but allow this loading to be made severe enough to cause fatigue within a reasonable time. Very little detailed work has been done to characterise the initiation and early growth of fatigue cracks in multi-layer and multi-phase bearing materials systems. In this study initially no attempt has been made to model the service loading, rather it is proposed to investigate the fundamental fatigue behaviour of the bearing system in a simple well characterised stress state. To achieve this the test matrix comprises simple three point bend tests on flat specimens (80mm by 20mm by 2mm) of the multi-layer material produced just prior to bearing forming (thus testing material in a similar condition to that in the bearing). Flat strips were preferred over actual bearings for short crack analysis since the stress state is easier to model and both sample preparation and crack monitoring are facilitated by a flat sample. Limited amounts of monolithic bearing lining material, produced by a similar processing route as that experienced by the bearing lining, was available as thin sheets of 0.5mm by 180mm by 60mm. Some centre cracked tension (CCT) long crack testing was carried out to provide appropriate long fatigue crack growth data.

Fatigue crack testing

Insufficient monolithic material existed to allow the full da/dN-ΔK curve to be established under constant load conditions within one CCT sample. Precracking was carried out at $\Delta K = 3MPa\sqrt{m}$ to a length of 2mm. The load was then incrementally increased in $1MPa\sqrt{m}$ steps from 3 $MPa\sqrt{m}$ to 9 $MPa\sqrt{m}$ after 1mm of crack growth at each ΔK range. The test was performed using an Instron 8502 servo-hydraulic at R=0.1 and at a frequency of 10Hz, using D.C.P.D. for crack monitoring. Short crack tests on the flat bearing strips were performed at the same R-ratio and frequency using an Instron 8501 servohydraulic machine. Cycling was periodically interrupted and acetate replicas taken of the top surface to monitor crack initiation and growth. Since multiple crack initiations were expected [1] three point bend tests were used to reduce the area of likely initiation and thus the area required for crack monitoring, thus making the subsequent analysis easier. Before testing the surface of the Al lining material was polished back to a 0.25μm finish to give the same sample thickness as a finished bearing (~1.81mm) and also to provide a good surface finish for replication. It was found through experimentation that to initiate fatigue cracks on the bearing lining surface of the flat samples, it was necessary to test at a load level such that the maximum stress in the bearing lining was apparently well above the yield stress. Such loading causes both the steel layer and the lining to behave plastically, and hence fatigue tests cannot be run to final failure since the accumulated plastic strain in the steel causes gross overall deformation of the sample prior to this. Testing above the yield stress invalidates compound beam theory as a reliable method of calculating maximum surface stress in the sample, instead a simple elasto-plastic finite element model was used to predict this stress in the bearing lining for a given load. This model was created using the ANSYS5.4 code. The model uses 540 8 node quadrilateral

elements to model a section of the bearing material in two dimensions. Only the lining and backing materials were modelled, the interlayer was ignored since its properties are very close to those of the lining material.

Plasticity was introduced by using a full isotropic strain-hardening curve for the lining material. Only yield stress and tangent modulus data were available for the steel backing layer. The model used point loads applied directly to key-points. An investigation was performed to appraise the effect of incorporating the Hertzian contact between roller and specimen. The effect on maximum surface stress was found to be very small and the non-linear nature of the contact elements used considerably increased the computational expense of the model, hence this approach was discarded.

After testing failed samples were examined in the SEM and optical microscopy carried out on sectioned samples, which were polished to a 0.25 μm finish.

RESULTS

Material characterisation

Optical microscopy on polished samples of lining alloy revealed it to be a multiphase material. The Sn and Si secondary phases exist as two discrete distributions. The Sn phase tends to exhibit a discontinuous recticular distribution, whilst the Si distribution is spheroidised and often seen associated with the Sn phase. A micrograph of the lining alloy microstructure is shown in figure 1.

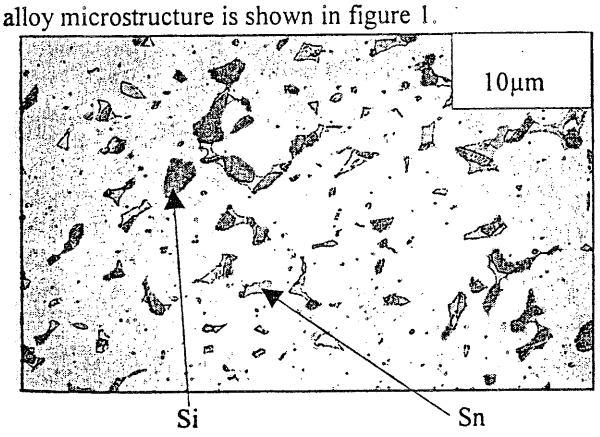

Figure 2: Section of bearing lining alloy microstructure after polishing

Centre cracked tension test results

Incrementally increasing the load throughout the test allowed limited data to be collected over the ΔK range 3-9MPa√m as shown in figure 2. A lot of scatter is observed, obvious load transient effects were observed whenever the load was increased, with initially greatly accelerated crack growth. This could be a real effect due to underload effects or could be a feature of the crack monitoring method via electrical closure. Individual long crack tests will be carried out under constant load conditions to identify long crack growth behaviour better at the lower and higher ΔK ranges as more monolithic material becomes available, but this initial test has helped to identify the long crack fatigue regime

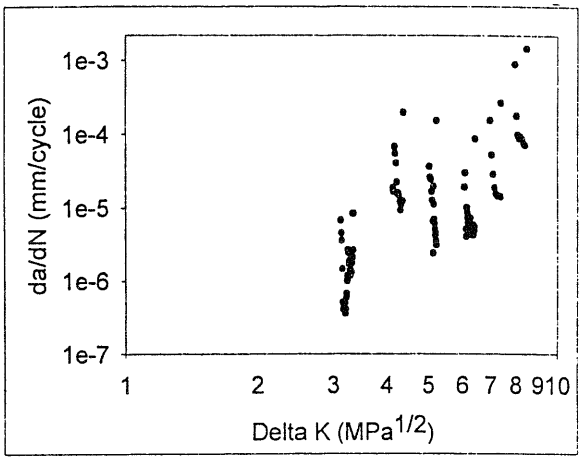

Figure 2: CCT long crack test results

Short crack test results

In order to initiate fatigue cracks in the polished samples it was found necessary to test at stress levels above yield stress. The finite element model predicted a top surface tensile stress of 175% of yield stress or 73% of ultimate tensile stress given the applied load. This model also allowed investigation of the stress field through the sample thickness as well as evaluating the peak stress at the surface of the sample

Cracks were seen to initiate at multiple sites on the bearing surface within 500 cycles as shown in figure 3. Initiation sites appear to be largely associated with the interface between the matrix and Si phase rather than the Sn phase as Shenton et al [1] has reported

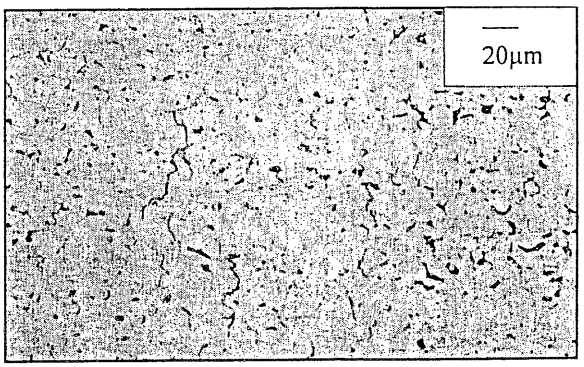

Figure 3: Multiple crack initiation sites on sample surface

An SEM micro-graph of an initiation site is shown in figure 4. Several cracks have initiated from, and are propagating along the interface between the Si phase and the matrix, causing the Si to practically de-cohere from the matrix. It is interesting to note that these small cracks are propagating parallel to the global applied tensile axis as well as perpendicular to it, indicating a locally complex stress state.

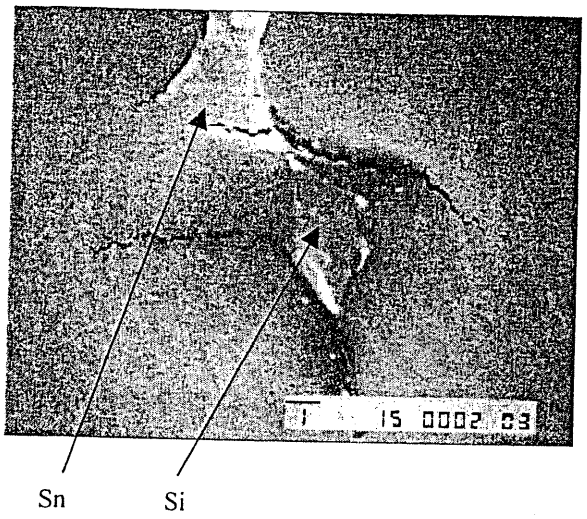

Figure 4: Crack initiation site showing de-cohered Si phase

The early growth rate of these cracks was extremely rapid and microstructurally dependent, the crack tip appearing to preferentially propagate through the soft Sn phase or along the interfaces between Si phases and the matrix, as is shown in figure 5.

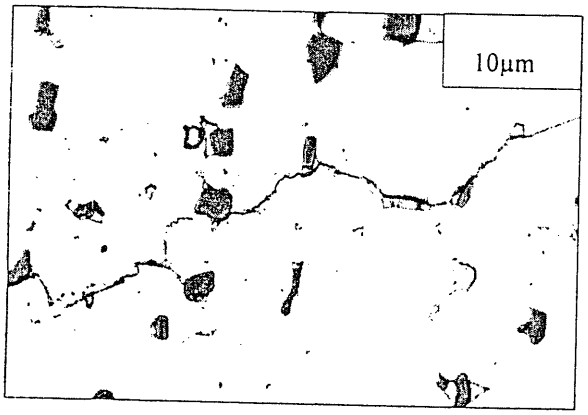

Figure 5: Microstructurally dependent crack path - showing propagation through Sn phases and along Si-Al interfaces

Clusters of micro-cracks coalesced rapidly to form larger cracks (typically after 40,000 cycles), The crack growth rate of these larger cracks dropped off markedly or indeed arrested entirely, once they reached a top surface crack length of ~0.73mm; (c.f. lining thickness of 0.3mm). A micrograph of the material surface after 60,000 cycles is shown in figure 6; the larger cracks have formed through coalescence. It was not possible to continue the test until final failure from these cracks, since the accumulated plastic strain in the steel layer caused the sample to permanently deform.

A sample was sectioned after testing to investigate the sub-surface crack behaviour. It was found that upon reaching the pure Al interlayer, rather than propagating into the steel, the crack bifurcates and grows along the interlayer.

This type of crack bifurcation has been observed by prior experimental researchers [1] in accelerated rig testing failures. An example of the bifurcation is shown in figure 7.

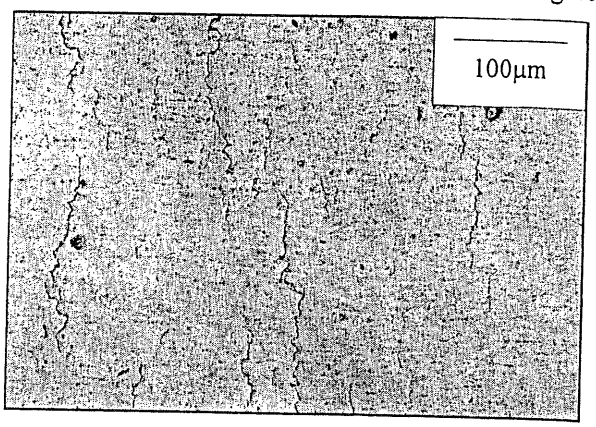

Figure 6: Large dominant cracks formed after multiple crack coalescence

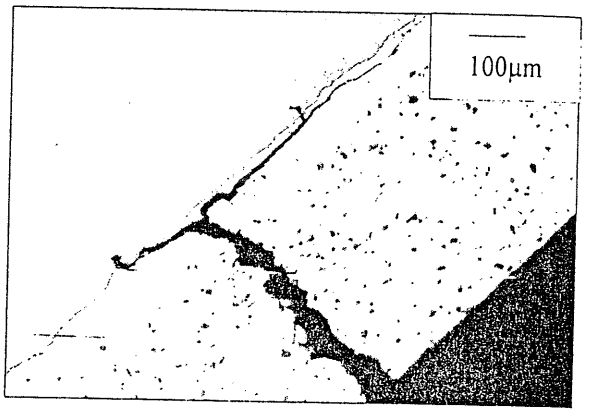

Figure 7: Sub-surface fatigue crack behaviour showing crack bifurcation at the interlayer

Short crack ΔK levels were calculated using the equation proposed by Scott and Thorpe [2]. These were evaluated for the surface condition and assuming a penny shaped crack, the data are presented in figure 8. However it should be noted that the short cracks are growing under elasto-plastic conditions, and hence the use of ΔK is questionable as LEFM conditions are clearly not maintained. ΔK has been used as a correlation parameter for purposes of comparison with long crack data (in accordance with other short crack studies in the literature)

It appears that the short cracks grow at far lower ΔK levels than the long crack, and that the individual crack growth rates accelerate and decelerate, despite experiencing a constant applied load range throughout the test.

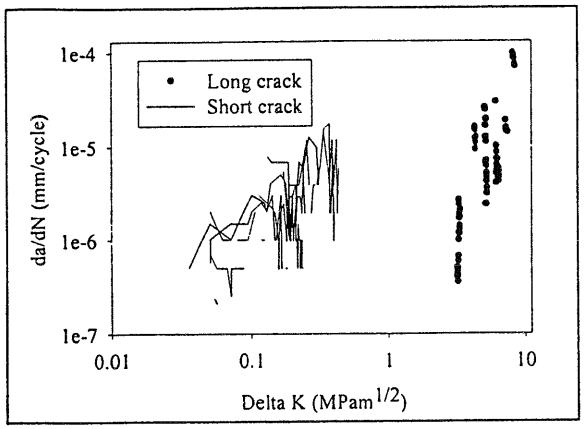

Figure 8: Comparison of long and short crack growth rates in bearing lining material

Fractography

In order to better understand the behaviour of a fatigue crack propagating in the lining material the fracture surface of the CCT sample was examined using scanning electron microscopy. It was found that at low ΔK the fracture surface was rough with the secondary phases clearly evident. At higher ΔK the fatigue fracture surface is much smoother, classical striations are present in the matrix material whilst the secondary phases are less evident. Micrographs are given of the fracture surface near threshold at $\Delta K = 3MPa\sqrt{m}$ and at $\Delta K = 5MPa\sqrt{m}$ in figures 9 and 10 respectively.

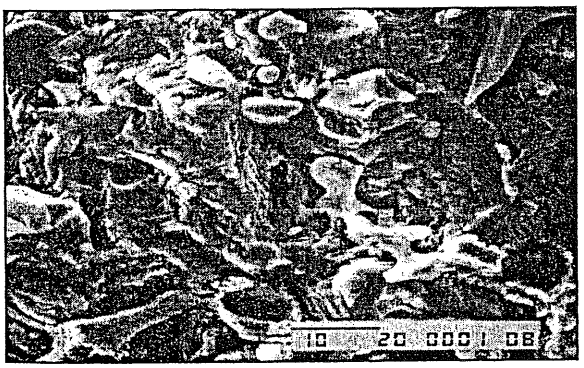

Figure 9: Fracture surface of monolithic lining alloy produced at $\Delta K = 3MPa\sqrt{m}$

Figure 10: Fracture surface produced in monolithic lining alloy at $\Delta K = 5MPa\sqrt{m}$

MICROSTRUCTURAL FINITE ELEMENT MODEL FORMULATION

A finite element model was developed to further assess preferential initiation sites in the lining material. The lining material microstructure was modelled using a 2D embedded cell approach, in which the real inhomogeneous material is approximated by a model material comprising a core region containing the discrete phase arrangement embedded within a larger region to which far field loads are applied. This approach was taken since it was felt that the periodicity constraints of a unit cell approach would lead to a very poor approximation of such a naturally non-periodic microstructure unless the unit cell was made very large.

The core region where the material is modelled as discrete phases must be large enough to be statistically representative. This may not be the case in the model presented here. This model is a preliminary attempt and the core region was judged to be fairly representative of the overall microstructure by the authors. Possible future methods for ensuring the relevance of the core region are discussed later in the paper. The core region selected was a small area of microstructure containing a few small cracks that had just initiated (hence the presence of the crack will not have significantly distorted the spatial arrangement of the discrete phases prior to crack initiation); this is shown in Figure 11. The secondary phases within this core region were approximated as 18 sided polygons (maximum available to a single discrete area in the ANSYS code).

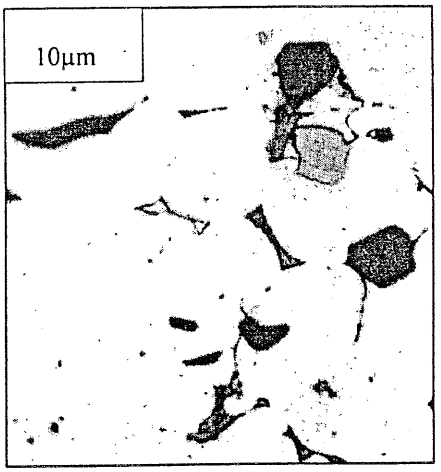

Figure 11: Area of lining material microstructure selected as core region

The embedded region was meshed using 6512 8 noded iso-parametric elements in plain stress. This mesh was refined near to the interfaces between secondary phases, and between secondary phases and the matrix, as is shown in figure 12. Perfect bonding between phases and the matrix was assumed and no attempt has been made to model the movement between phases if this occurs. An embedding region 25 times the size of the core was used to distribute the far field loading sufficiently (this is in line with the work of Dong et al [3]). The outer embedding region was meshed

more coarsely than the core with only 400 elements to reduce the computational expense of the overall model.

Isotropic plasticity was used throughout the model. As in the model for load prediction, a full hardening curve was used for the lining alloy embedding material, but simple yield stress and tangent modulus data was used for the Al matrix and secondary phases. Since no kinematic hardening data was available it was not possible to create a dynamic solution and consider the effect of fatigue; rather the model simulates the first load step only. This means effects of accumulated plastic strain, etc. can not be considered by this model given its current inputs. The model was loaded via a small uniform nodal displacement along the edge of the embedding region, effectively a simple tensile load as shown by the arrows in Figure 12. This uniaxial loading was judged to be representative of the top surface loading in a bend test, since the surface area considered is small enough for shear loading to be ignored. The model was solved using the ANSYS 5.4 finite element code.

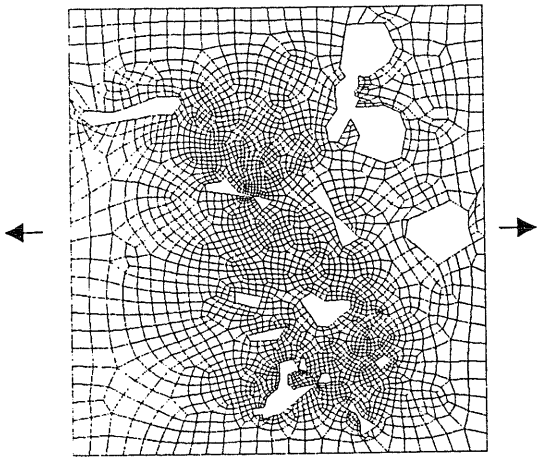

Figure 12: Finite element mesh of core region, Al matrix elements only

MODEL RESULTS

The model revealed the presence of high stress concentrations at the interfaces between the Si phases and the Al matrix. These results from the model appeared to be consistent with experimental observations, with cracks initiating from the regions of predicted stress concentration. (It should also be noted that the model predicted stress concentrations at a few points where no crack initiation occurred).

Figure 13 shows the stress field around a pair of Si phases joined by a Sn phase. A high stress concentration has been generated between the two Si particles at the interface between matrix and Sn phase. Also a secondary smaller stress concentration exists at the interface between the Si phase and the matrix. Comparison with the original microstructure shows that this is where the crack initiated. Figure 14 shows a stress concentration associated with a single Si phase separate from any Sn phase.

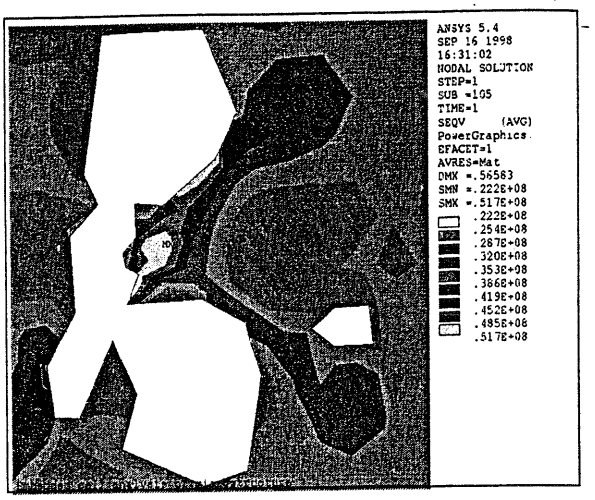

Figure 13: Stress concentration evolved at interface between Si and Sn secondary phases

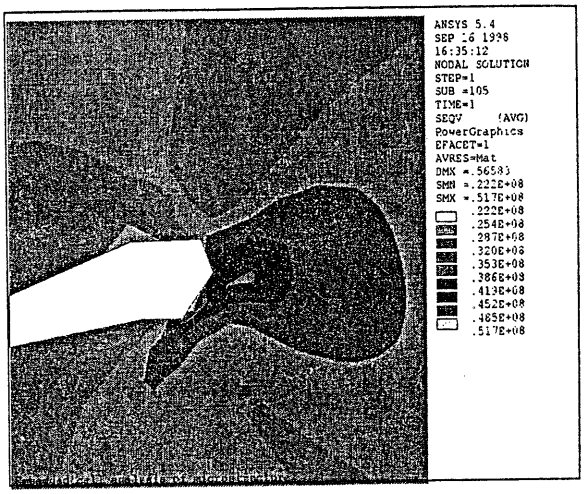

Figure 14: Stress concentration associated with single Si secondary phase

The stress concentration shown in figure 16 is present at the interface between an isolated Si phase and the matrix. Comparison with the original microstructure again showed that a crack had initiated from this point.

DISCUSSION

Short cracks initiated at multiple points on the surface of the specimen, primarily at the interfaces between the Si secondary phases and Al matrix. It is thought that this is due to the large difference in compliance between these two phases. If this is the case one would expect cracks to also initiate at interfaces between Sn and Si particles, since the compliance ratio is even higher between these phases. However this has not been observed in experimental specimens. Shenton et al [1] also observed fatigue crack initiation in this alloy at slip bands, no such initiations of this type were observed in the current work. The microstructural finite element model showed that high stress concentrations

were produced at the type of features seen to produce fatigue crack initiations in experimental specimens. It appears that the boundaries between Si phase and the matrix are very weak, this may mean that the assumption of perfect inter-phase bonding made when formulating the microstructural model is invalid.

Initial short fatigue crack growth was found to be very rapid and microstructurally dependent. The crack path is highly tortuous; the crack appears to propagate preferentially toward the soft Sn phase and along the Si-matrix interfaces. This observation is partially supported by the work of Padkin et al [4] who suggested that particles having a modulus lower than the matrix will tend to attract and accelerate cracks. Short cracks either arrest soon after initiation or coalesce and continue growing rapidly. The fatigue crack growth rate is seen to drop markedly or indeed arrest entirely when the crack reaches a critical length of approximately twice the lining thickness (~0.7mm). If a penny shaped crack is assumed then this drop in crack growth rate corresponds to the point at which the lining material is cracked through and the crack reaches the interface between lining and backing. From sectioning studies it is seen that when this occurs the crack bifurcates and grows along the interlayer, producing a complex 3D shape. This degree of crack deflection will cause a large increase in extrinsic crack tip shielding, with a corresponding reduction in crack driving force and hence growth rate, as shown by Suresh et al [5]. It has also been shown that crack deflection and retardation occur when a crack propagating in a softer material approaches an interface with a harder material, and this has been linked to a reduction in local normal and hydrostatic stress, as shown by Sugimura et al [6]. Hence continued crack growth on the initial path becomes progressively less favourable as the crack tip plastic zone nears the interface. This effect was demonstrated [6] using a finite element model to evaluate the J integral around a crack tip as it approached a bi-material interface. It was found that the effective J at the crack tip could become smaller than the remotely applied J as the crack tip plastic zone impinged on the interface. Consequently the crack tip is shielded from remote loads, hence reducing the crack growth rate.

Examination of the fatigue fracture surface produced during the long crack test showed pronounced differences with rising ΔK. At low ΔK-levels, near-threshold, the fatigue fracture surface appears rough, and the secondary phases are evident on the surface, indicating that the crack is preferentially seeking out these phases, and that the crack path itself is tortuous. This tallies with the observations of the short crack path behaviour, where cracks propagate preferentially toward the soft Sn phase and along the Si-matrix interfaces. The short cracks appear to grow at much lower ΔK levels than the long crack, but the elasto-plastic conditions in the short crack case make direct comparison with the long crack data problematic. In the long crack case, at higher ΔK, the secondary phases are far less evident in the fracture surface, which is much smoother and displays classical striations. This indicates that it is only at lower ΔK levels that the crack seeks out the secondary phases.

SUMMARY AND CONCLUSIONS

The initiation and early growth of fatigue cracks in this lining alloy is highly dependent on its multiphase microstructure. Initiation occurs primarily at the interface between Si phases and the Al matrix. At low ΔK levels cracks are seen to propagate preferentially along Si-Al interfaces or through Sn phases. Preliminary modelling of the microstructure appears to indicate that stress concentrations exist at these initiation sites. It has been shown that the multi-layer material system used in this type of shell bearing leads to a large reduction or even arrest in crack growth once the lining material is cracked through. This has been attributed to a large increase in crack tip shielding due to crack bifurcation.

FURTHER WORK

Further quantitative analysis of the secondary phase distributions is planned using tessellation approaches [7] to characterise the local microstructural features around fatigue initiation sites and to evaluate fatigue crack path preferentiality. This will also allow a better representation of the relevant microstructure for the embedded cell approach to be determined.

ACKNOWLEDGEMENTS

The authors would like to thank EPSRC and Dana Glacier Vandervell for financial support throughout the duration of this project.

REFERENCES

1. P. Shenton and C. Perrin, *Private communication*, Dana Glacier Vandervell.
2. P.M. Scott and T.W. Thorpe, Fat. Engng. Mat. Struct, **4**, 291 (1981)
3. M. Dong and S. Schmauder, *Modelling of metal matrix composites by a self consistent embedded cell model*, Acta Mater., **44**, 2465-78, (1996)
4. A.J. Padkin, M.F. Brereton and W.J. Plumbridge, *Fatigue crack growth in two phase alloys*, Mater., Sci..& Tech., **3**, 217-223 (1987).
5. S. Suresh & C.F. Shih, *Plastic near tip fields for branched cracks*, International journal of fracture, **30**, 237-59 (1986)
6. Y. Sugimura, P.G. Lim, C.F. Shih and S. Suresh, *Fracture normal to a bimaterial interface: Effects of plasticity on crack tip shielding and amplification*, Acta Met., **43**, 1157-1169, (1995)
7. J. Boselli, I. Sinclair, P.J. Gregson and P.D. Pitcher, *Scripta Mater.*, **38** (5), 839-844, (1997)